



# Journal of Applied Sciences

ISSN 1812-5654

**science**  
alert

**ANSI***net*  
an open access publisher  
<http://ansinet.com>

## An Agent-Based Approach for Regional Forest Fire Detection using MODIS Data

<sup>1</sup>S. Movaghati, <sup>1</sup>F. Samadzadegan and <sup>2</sup>A. Azizi

<sup>1</sup>Department of Geomatics Engineering,

<sup>2</sup>Centre of Excellence for Disaster Management, Department of Geomatics Engineering,  
College of Engineering, University of Tehran, Iran

---

**Abstract:** In this study, we propose an agent-based approach for adaptive regional forest fire detection using MODIS data. It utilizes the tests used in MODIS version 4 contextual fire detection algorithm to determine agent behavioral responses. To do so, initially, a collection of autonomous agents will be distributed at a number of pixels in the considered image with high potential of being a fire pixel. These pixels are pre-selected based on brightness temperature and NDVI values of a given pixel with respect to those of its surrounding pixels rather than fixed threshold values. Performance of the proposed algorithm was compared with MODIS version 4 contextual fire detection algorithm and ground-based measurements. The results show high potential of the proposed method to be applied for automatic forest fire detection at regional scale.

**Key words:** Multi-spectral remote sensing, regional forest fire detection, spatial information, agent-based approach, MODIS

---

### INTRODUCTION

To date, several algorithms have been proposed for fire detection using remote sensing data. Generally, the presented algorithms based on single-date remote sensing imagery are classified as either fixed threshold or contextual (Li *et al.*, 2001). In comparison, contextual algorithms are more flexible than the former, because they are self-adaptive and automatically detect fires under different conditions (Giglio *et al.*, 1999; Ichoku *et al.*, 2003; Li *et al.*, 2001, 2005). For example, the MODIS contextual fire detection techniques are planned to be fully automated for operational daily, global fire monitoring (Giglio *et al.*, 2003; Justice *et al.*, 2002; Kaufman *et al.*, 1998). However, in contextual algorithms, selection of fixed threshold values for identifying potential fire pixels (a primary classification for elimination of obvious non-fire pixels) is counted as a weakness for regional fire detection in which detection of small fires is important too; inadequate fixed threshold values may produce either commission or omission errors (Csiszar *et al.*, 2003; Cuomo *et al.*, 2001; Giglio *et al.*, 2003; Li *et al.*, 2001, 2003; Wang *et al.*, 2007). To solve this problem some efforts have already been carried out (Wang *et al.*, 2007). In this study, we propose an agent-based approach for regional forest fire detection using MODIS data.

Autonomous agents are systems that inhabit a dynamic, unpredictable environment in which they try to satisfy a set of time dependent goals or motivations (Maes, 1994). Since last decade, some efforts have been done for application of agents in image processing. For example, algorithms represented by Liu and Tang (1998, 1999) are agent-based approaches for image segmentation. In these studies, agents operate directly on the individual pixels of a given image. The behavioral patterns of the agents are pre-defined and will trigger their local stimuli that come from evaluation of some criteria in their neighboring regions. The agents exhibit some of the following reactive behaviors: breed offspring agents, move to adjacent pixels, leave a label, or vanish in the image. Compared with conventional methods, agent-based approaches have some advantages such as being adaptive to locality, reliable in performance, less sensitive to the noise and easy to represent and implement repeated again and again in literatures (Keshtkar and Gueaieb, 2006; Liu and Tang, 1998, 1999). To benefit from abovementioned advantages, we represent an agent-based approach for forest fire detection using diurnal MODIS data at regional scale. It is based on MODIS version 4 contextual algorithm (Giglio *et al.*, 2003) but there is no need to set any fixed threshold value for selection of potential fire pixels.

**MATERIALS AND METHODS**

**Satellite data set:** Remotely sensed data used to detect active fires are MODIS level 1B radiance product (MOD02) and geolocation data set (MOD03). The MODIS data used for this study covers the period from 24 July 2006 to 27 July 2006 (3 days) for our study area, Kermanshah Province (Table 1). The TIR band data were converted into brightness temperature using inverse Planck function. Moreover, the reflectance values are computed from visible and NIR bands. The bands used in our study are shown in Table 2. In addition, the view and solar zenith/and azimuth angle values and land/sea mask were obtained for each image. NDVI values were also calculated for each image.

**Auxiliary data:** The ground observations were provided by Forest, Range and Watershed Management Organization using GPS (Table 3). Standard forms are used for documentation of when and where fires occurred. These fire reports are based on ground observations and include the fire number, location, size and burning period.

**Proposed agent-based approach for regional forest fire detection:** The flowchart of this proposed algorithm is shown in Fig. 1. The proposed algorithm is composed of the following steps: cloud and water masking, identification of potential fire pixels, agent initialization and searching and labeling active fire pixels. In present

approach, agents operate directly on the individual pixels of a given image. Initially, they are inhabited in potential fire pixels selected using brightness temperature values in 4 and 11 μm bands (depicted by  $T_4$  and  $T_{11}$ , respectively) and NDVI values of a neighboring region. They sense the neighboring pixels and check some criteria based on tests used in MODIS version 4 contextual algorithm (Giglio *et al.*, 2003) to detect forest fire pixels. The agents can self-reproduce, diffuse and vanish during the course of interacting with a given image.

**C Cloud and water masking:** The 1 km land/sea mask contained in MODIS geolocation data set is used to exclude water pixels. Cloud detection is based on the technique used in the MODIS version 4 contextual algorithm (Giglio *et al.*, 2003)

**C Identification of potential fire pixels:** Using  $T_4$ ,  $T_{11}$  and NDVI values, potential fire pixels are selected from MODIS images in a different manner compared to conventional approaches. The proposed method is based on local variation of  $T_4$ ,  $\Delta T = T_4 - T_{11}$  and NDVI values of pixels in a  $n \times n$  window ( $n = 3$ ) for selection of potential fire pixels among all the cloudless and non-water pixels. It does not require any fixed threshold value. Indeed, after cloud and water masking (Giglio *et al.*, 2003), a pixel is identified as a potential fire pixel if it satisfies the following conditions:

$$T_4 = \text{Max}(T_{4w}) \tag{1}$$

$$\Delta T = \text{Max}(\Delta T_w) \tag{2}$$

$$\text{NDVI} = \text{Min}(\text{NDVI}_w) \tag{3}$$

where, subscript w indicates local window centered in the supposed pixel. As a result,  $N_{\text{PFP}}$  pixels are detected as potential fire pixels.

Test 1 and 2 are based on the fact that if a forest fire happens in an area, it will bring rapid changes in brightness temperature value of the corresponding pixel compared to its surrounding (Byun *et al.*, 2005). The sharp contrast between target, here fire and background

Table 1: Specifications of MODIS imageries used

Image No.	Date	Time (GMT)	
		Start	End
1	2006-07-24	07:42:44	07:45:28
2	2006-07-26	07:30:46	07:33:17
3	2006-07-27	08:13:19	08:16:16

Table 2: MODIS bands used in this study

Band No.	Band width (μm)
1	0.620-0.670
2	0.841-0.876
7	2.105-2.155
21	3.930-3.989
22	3.930-3.989
31	10.780-11.280
32	11.770-12.270

Table 3: Specifications of ground based measurements

Region	Date	Area (ha)	Spatial coordinate of fire		Time (Local)	
			Latitude	Longitude	Start	End
Sahneh, Bide Sorkh Defile	2006-7-26	15	34:26:10 N	47:28:51 E	16:30	18:30
Eslam Abad Gharb, Haroon Abad	2006-7-26	5	34:43:00 N	46:33:00 E	13:00	15:00
Eslam Abad Gharb	2006-7-27	10	34:05:00 N	46:31:00 E	14:00	20:00
Salase Babajani	2006-7-27	1	34:41:16 N	46:13:12 E	16:30	17:20
Gilane Gharb	2006-7-27	20	-	-	17:00	20:30

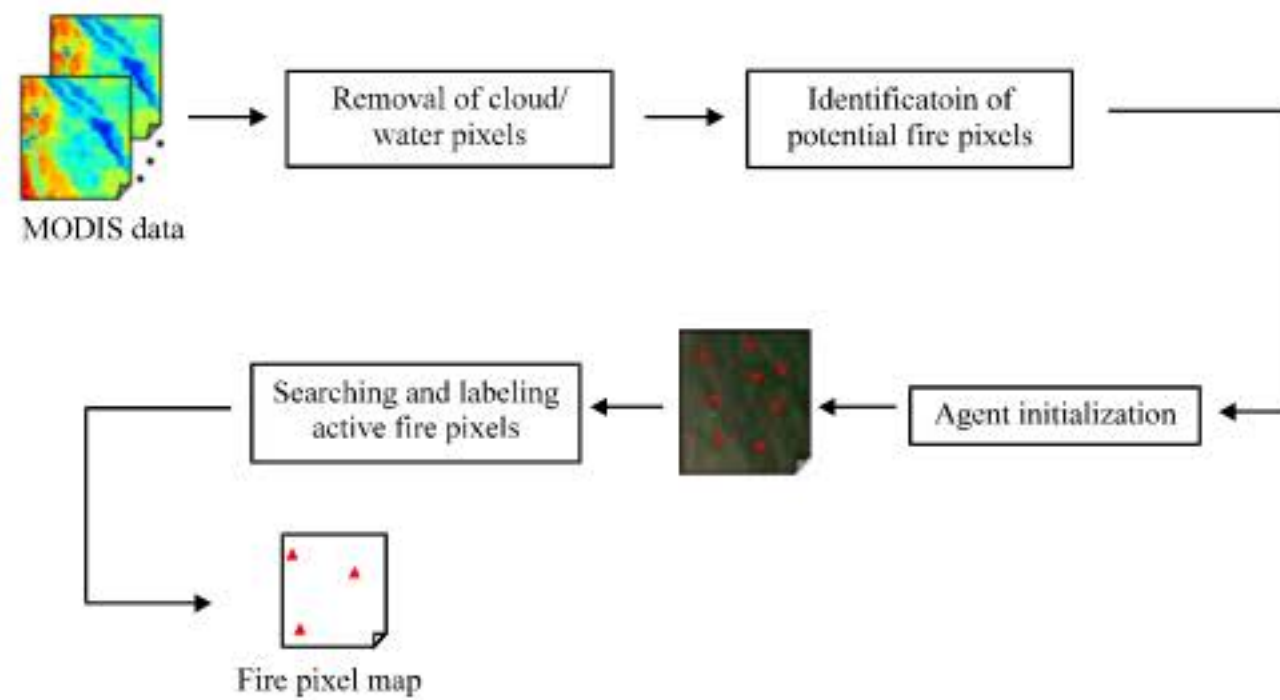


Fig. 1: The flowchart of the proposed algorithm

helps active fires to be reliably detected even when the fire covers small fractions of a pixel (Byun *et al.*, 2005; Lentile *et al.*, 2006). In addition, owing to Wien's displacement law, the brightness temperature of a fire pixel in MIR bands, e.g., 4  $\mu\text{m}$  band ( $T_4$ ), change significantly compared to that of in TIR bands, e.g., 11  $\mu\text{m}$  ( $T_{11}$ ), (Byun *et al.*, 2005), whereupon the difference between brightness temperature values of 4 and 11  $\mu\text{m}$  bands ( $\Delta T$ ) is a main parameter to distinguish between fire and non-fire pixels in a given neighborhood. Also, test 3 is based on the fact that at the spatial resolution of most satellite sensors (pixel size  $> 30$  m), when vegetation is burned, the surface reflectance in visible to NIR region (i.e., 0.4-1.3  $\mu\text{m}$ ) decrease significantly (Lentile *et al.*, 2006). Moreover, Robinson (1991) showed that pixels containing hotspots and their nearest neighbors, tended to be less green than the general background. They interpreted it as fire damage to vegetation. In other words, NDVI value of an active fire pixel is less than those of its neighboring pixels. Using NDVI values in combination with brightness temperature values in tests 1-3, we take into consideration the nature of fires in forest lands, not any hot object.

**C Agent initialization:** The given image is considered as a grid for a class of autonomous agents, i.e., fire agents (Fig. 2). As shown in Fig. 2,  $T_4$ ,  $\Delta T$ ,  $\rho_{0.65}$ ,  $\rho_{0.86}$ ,  $\rho_{2.1}$ , land/sea mask and  $\theta_g$  are the image features that will be used in next step. Here,  $\rho_{0.65}$ ,  $\rho_{0.86}$  and  $\rho_{2.1}$  are top of atmosphere reflectance values derived from MODIS 0.65, 0.86 and 2.1  $\mu\text{m}$  bands;  $\theta_g$  is sun glint angle. Initially, a group of  $N_{\text{FPF}}$  agents is distributed in the image. They are inhibited in potential fire pixels selected in the prior section. These pixels play an important role in fire detection. In fact, most of the fires are placed in these pixels which agents are initialized and the remaining of fire pixels are found by offspring agents generated around them

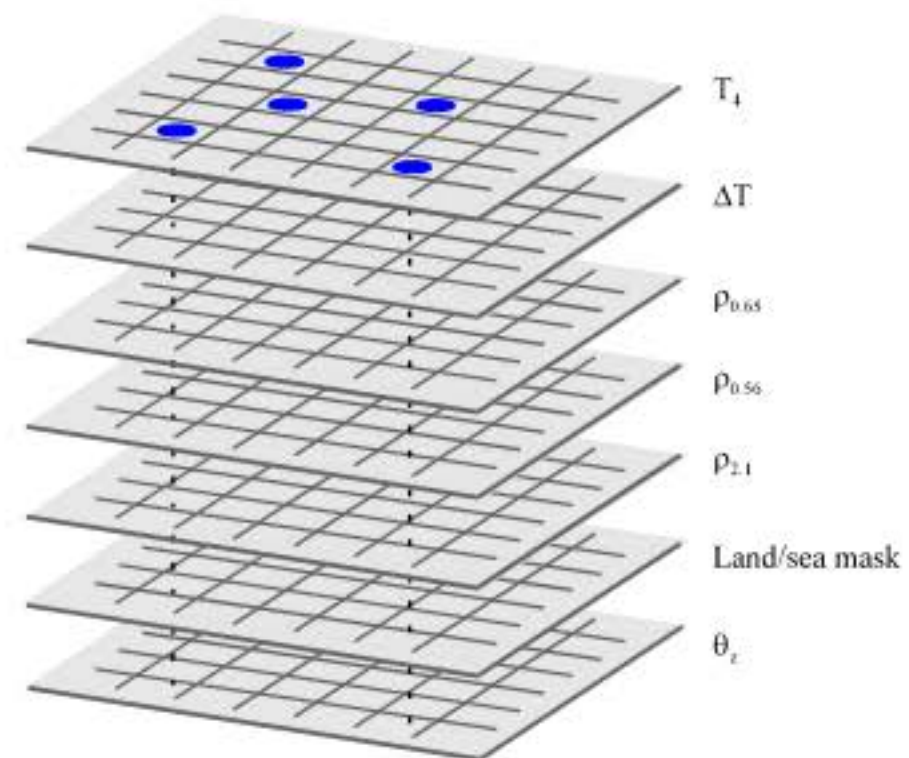


Fig. 2: Agent initialization, blue filled circles indicate agents

**C Searching and labeling active forest fire pixels:** For a given recognition goal, the task is to find an appropriate mathematical relation. In the present experiment, we used a series of tests (contextual tests and an absolute threshold test), designed for MODIS version 4 contextual algorithm (Giglio *et al.*, 2003), as the constraints that select and trigger the behavior of an agent at a pixel location for a neighboring region of radius  $R = 1$  to detect fires. The radius is increased to a maximum of 10, as necessary (Giglio *et al.*, 2003). The contextual tests use dynamic thresholds based on brightness temperature values of a given potential fire pixel and its neighboring. In addition, an absolute threshold test is used on a per-pixel basis. An agent will leave a marker at a daytime candidate fire pixel if the tests are satisfied, otherwise the agent will vanish (life span is set to  $\Delta = 1$ ). Also, three sets of tests are used to eliminate false alarms caused by sun glint, hot desert surfaces and coasts or shorelines as in (Giglio *et al.*, 2003)

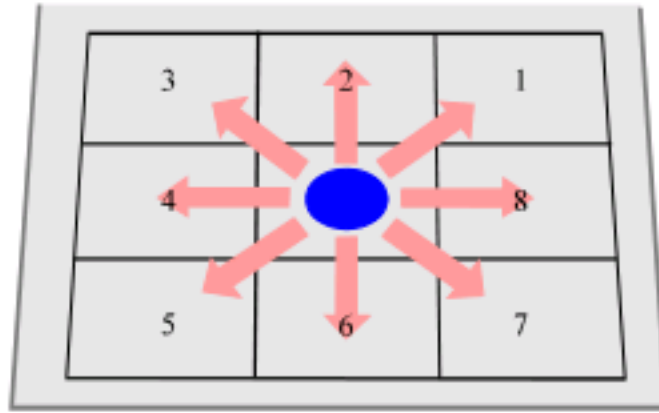


Fig. 3: An agent (indicated by a blue filled circle) and the directions for it to self reproduce within a neighboring region (indicated by pink arrows) when  $k = 1$

When a potential fire pixel contains no fire, it is not necessary to check its surrounding pixels. In such a case, an agent will not exhibit the behavior of moving to a new location within the neighboring region of the current location and vanish. If the fire size exceeds a pixel, it will be necessary to check the neighborhood of the considered pixel. To do so, the self-reproduction behavior generates a finite set of new agents near the pixel location labeled as a fire. The number of offspring agents reproduced at an active fire pixel is set to  $s = 2$ . The directions for an agent to self-reproduce within a neighboring region of radius  $k = 1$  are determined according to a vector. Each component of the vector expresses the ordering of having successful self-reproduction in an ascending mode if the respective behavior in a certain direction is performed. In fact, the vector ( $V$ ) can be written as follows:

$$V = \{v_1, v_2, \dots, v_8\} \tag{4}$$

where,  $v_i \in \{1, \dots, n\}$  and  $n = 8$  as shown in Fig. 3. Indeed,  $i$  is the ordering of a pixel in  $v_i$  direction in the sorted set of neighbors based on decreasing of  $T_4$  values.

**RESULTS**

The proposed algorithm was applied to the images shown in Table 1. Figure 4 shows the distribution of (a)  $T_4$ , (b)  $\Delta T$  and (c) NDVI values in one row from the image on July 24, 2006. In Fig. 4a-c, red circles indicate local maximum of  $T_4$ , local maximum of  $\Delta T$  and local minimum of NDVI values. Figure 4d shows the results after identification of potential fire pixels. According to field data (Table 3), the selected row in the image contains no fire. As can be shown in Fig. 4d, any pixel wasn't detected as a potential fire pixel. Figure 5a-c show those for one row from the image on July 27, 2006. According to field data (Table 3), there is a sub-pixel fire in the selected row.

Table 4: Attribute values for agent behavioral responses

Attribute	Description	Values
$k$	Radius of self-reproduction region	1
$\Delta$	Life span of agents	1
$s$	Number of offspring agents	2

As can be shown in Fig. 5d, this pixel was detected as a potential fire pixel. Figure 5a-d show how spatial information surrounding pixels can be used to select potential fire pixels instead of fixed threshold values. To detect forest fire pixels, initially a number of agents are inhabited on previously selected potential fire pixels in the images. The attribute values for agents are shown in Table 4. Since, agent initialization and selection of the direction for agents to self-reproduce are not done randomly, but based on spatial information, after a few directional movements they will find fire events.

We compared the performance of the proposed algorithm with the MODIS fire product (version 4). Figure 6a and b are results of the image 1 (Table 1) produced by the proposed algorithm and MODIS fire product. The image was taken on July 24, 2006 when there was no fire event to be reported (Fig. 6c, Table 3). As can be seen, both algorithms haven't detected any fire. This image was selected to test false alarm rate detected by the proposed algorithm. Figure 6d and e are the results of the image on July 26, 2006 when two fire events with 5 and 15 ha extent, respectively were reported by ground truth data (Table 3) shown in Fig. 6f. As mentioned in Table 3, the first one happened from 1:00 to 3:00 pm and the second one from 4:30 to 6:30 pm. According to the image acquisition time (morning), in relation to time of the reported fires, it is likely to miss these events. On the other hand, a single-pixel fire on the top is reported by both algorithms; another one was only detected by the proposed algorithm. For the latter pixel, because the  $\rho_{0.86}$  value is 0.3414, it is omitted in the MODIS contextual algorithm. In other words, selection of the threshold values for potential fire pixels (Giglio *et al.*, 2003), here threshold value of  $\rho_{0.86}$  (0.3) can cause omission errors. Although, we do not found any information about these fires in field data, they are likely to happen in non-forested lands e.g., pasture or farms and not reported. Indeed, according to Fig. 7a-d and 8a-d, these pixels are detected as potential fire pixels by the proposed algorithm. Also, considering images 1 and 3 with respect to image 2 (Table 1), these pixels have potential to be active fires. Referring to the first case, Fig. 9 and 10 show  $T_4$  and  $\Delta T$  values, respectively for a small area around the considering pixel which is indicated in the red rectangular on July 24, 26 and 27, 2006. In Fig. 9b, the  $T_4$  value of the given pixel was about 10 K greater than the surrounding pixels, but in Fig. 9a and c, the  $T_4$  value of the given pixel

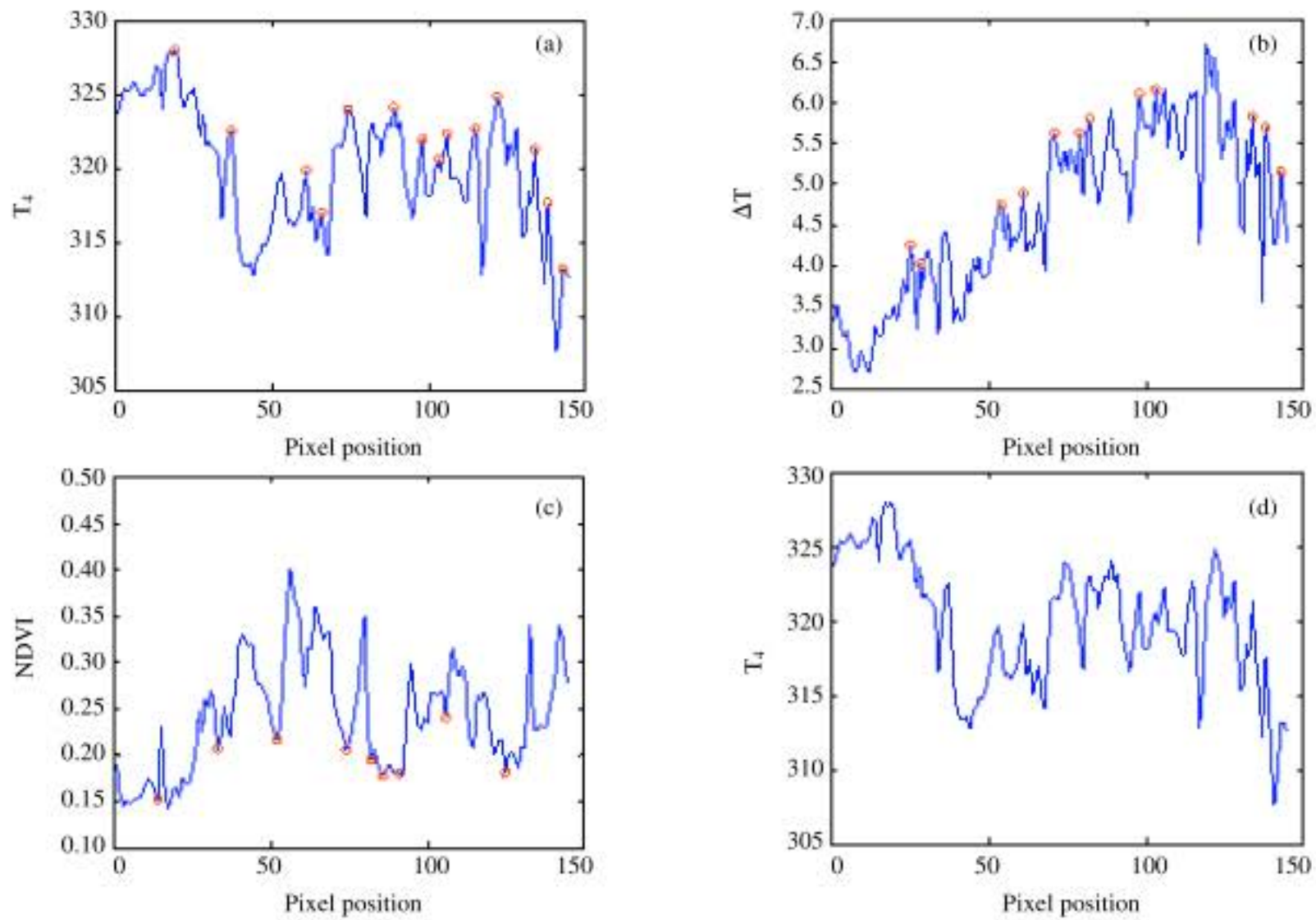


Fig. 4: (a) Local maximum of  $T_4$  profile, (b) local maximum of  $\Delta T$  profile, (c) local minimum of NDVI profile and (d) potential of fire pixels selected by the proposed algorithm (indicated by red circles). One row of data on July 24, 2006 is used

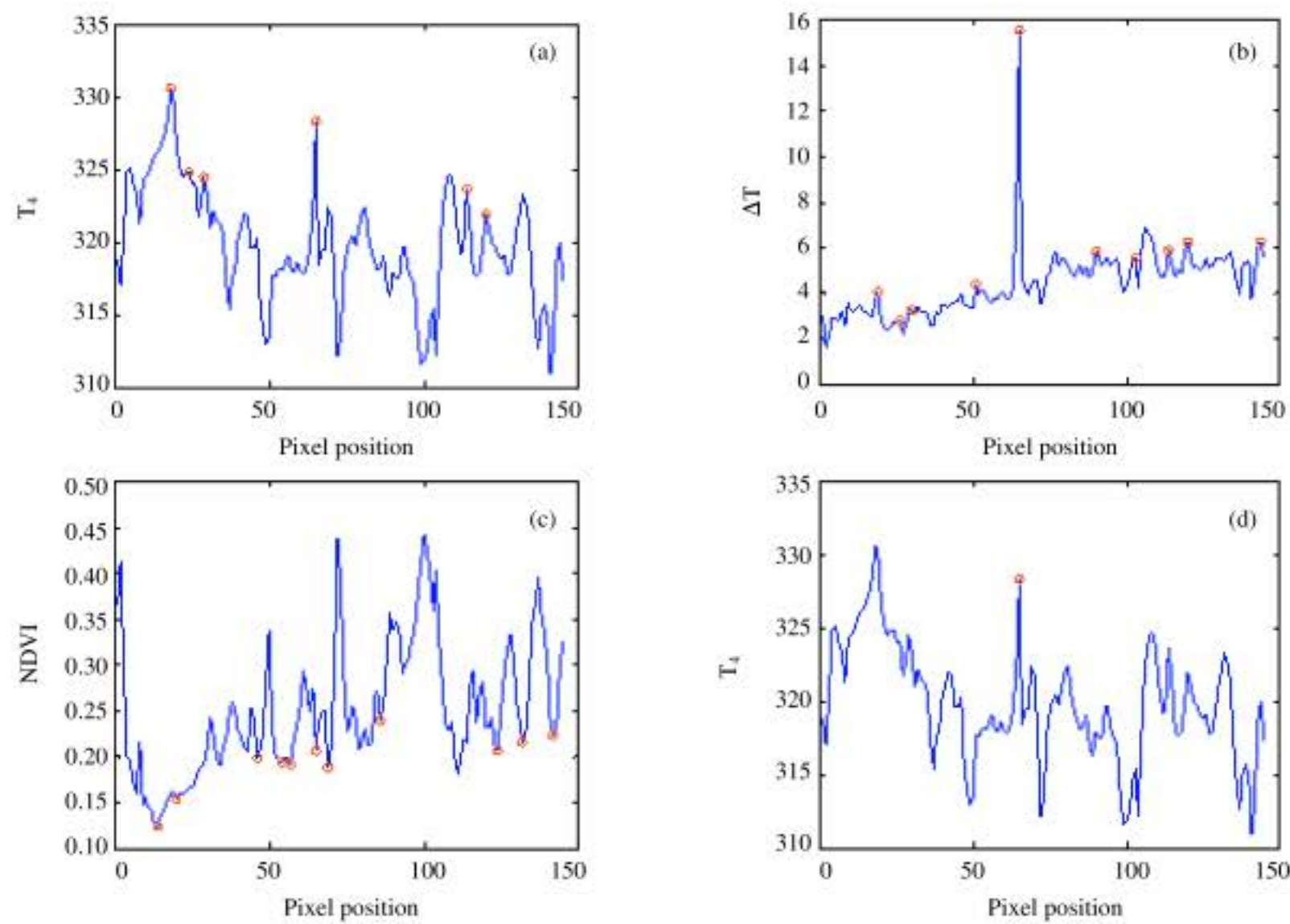


Fig. 5: (a) Local maximum of  $T_4$  profile, (b) local maximum of  $\Delta T$  profile, (c) local minimum of NDVI profile and (d) potential of fire pixels selected by the proposed algorithm (indicated by red circles). One row of data on July 27, 2006 is used

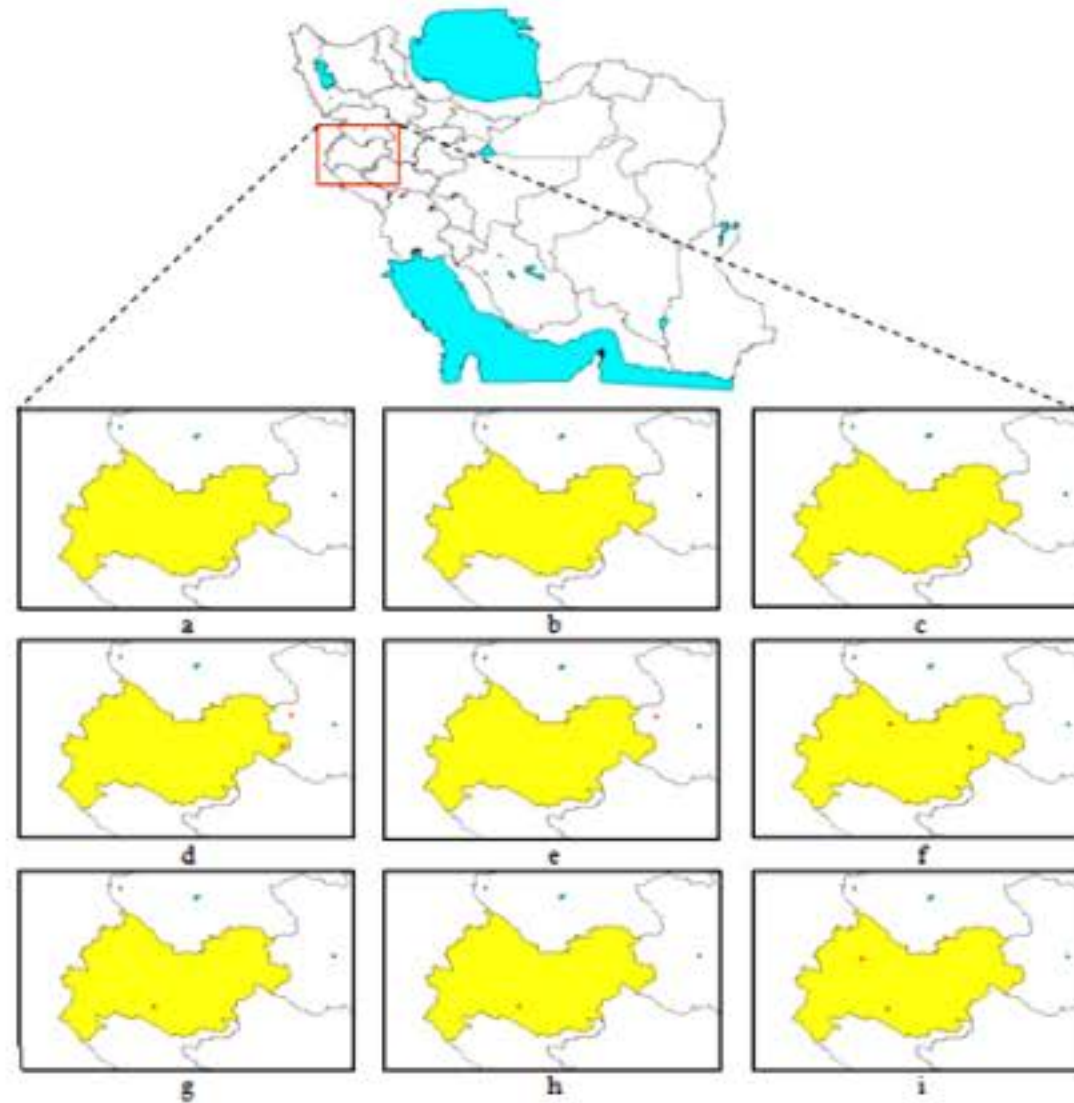


Fig. 6: Maps showing fire events detected over Karmanshah Province (highlighted) by the proposed algorithm, MODIS contextual fire detection algorithm (version 4) and ground based measurements on (a-c) July 24, (d-f) July 26 and (g-h) July 27, 2006, respectively. The red enlarged dots represents the fires detected

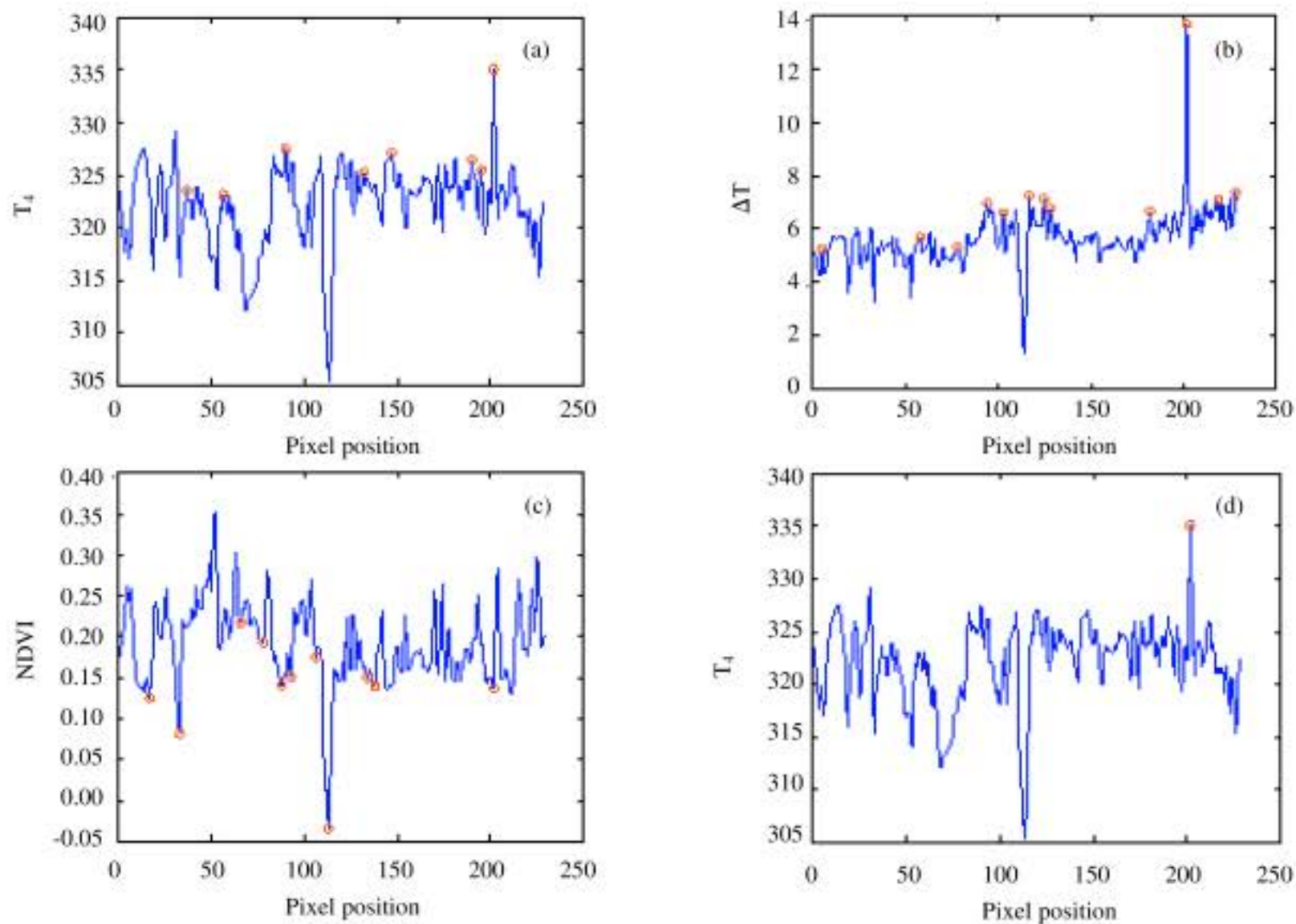


Fig. 7: (a) Local maximum of  $T_4$  profile, (b) local maximum of  $\Delta T$  profile, (c) local minimum of NDVI profile and (d) potential of fire pixels selected by the proposed algorithm (indicated by red circles). One row of data on July 26, 2006 is used

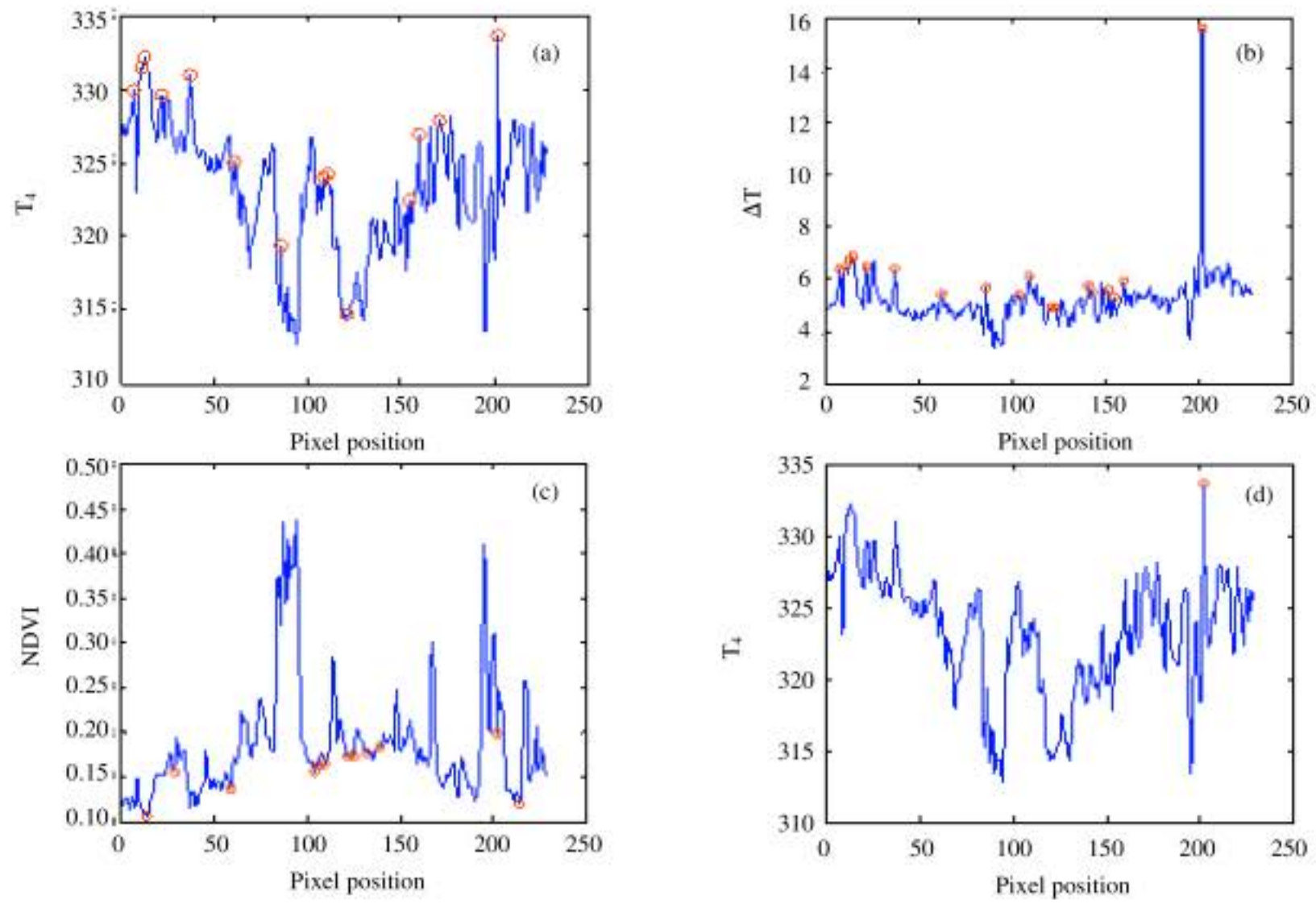


Fig. 8: (a) Local maximum of  $T_4$  profile, (b) local maximum of  $\Delta T$  profile, (c) local minimum of NDVI profile and (d) potential of fire pixels selected by the proposed algorithm (indicated by red circles). One row of data on July 26, 2006 is used

321.1392	320.7841	321.4395	323.2116	323.9835	325.4161	326.4303
323.2889	324.4908	325.1805	323.8131	325.2300	323.9695	323.4653
325.7089	327.3247	327.1237	326.3683	326.7248	322.2580	320.8872
326.9644	326.0830	327.6908	327.2355	328.1178	320.1161	323.8891
328.0970	327.9743	328.2048	327.9670	324.6624	322.1086	325.2525
329.5669	326.5193	324.4724	326.0500	325.7965	326.8947	328.0346
325.1693	321.7111	317.4726	317.4403	324.0857	327.0468	330.0629
<b>a</b>						
320.6385	320.9634	321.1354	323.4345	324.4701	325.0904	325.5255
322.3483	322.0558	324.4770	324.0997	324.8924	324.1170	324.8333
322.5185	324.1425	324.8288	325.8208	326.7129	323.7546	321.1316
323.6925	322.3836	324.3113	335.1636	325.2727	320.7726	323.1259
324.0462	323.5796	324.9808	328.6718	323.3446	323.5137	325.7688
323.4109	321.5444	321.1430	323.6290	326.1115	326.7366	328.2038
320.7496	317.6727	314.2709	318.3689	324.3551	326.8722	330.3751
<b>b</b>						
322.0508	321.0343	323.2758	321.9721	321.6055	321.9030	320.6180
320.6167	323.2164	323.6631	322.0656	323.7077	321.3267	320.9215
322.1282	322.1919	317.7869	321.1102	325.1152	323.8108	322.8169
321.6639	321.0862	322.1564	321.7855	319.1181	320.6052	318.9451
321.2236	320.9202	323.6443	322.1282	322.0447	322.2017	320.2264
320.8198	323.5078	321.7992	322.1687	324.8538	322.9214	322.4420
322.6336	319.3965	314.9358	315.6412	322.9669	324.0962	323.4310
<b>c</b>						

Fig. 9:  $T_4$  values around the first fire pixel detected by the proposed method indicated by a red rectangular on (a) July 24, (b) July 26 and (c) July 27 2006



4.5256	4.4389	4.7154	5.0499	5.1833	5.3991	6.1517
4.1267	4.3352	5.2817	4.6458	4.9668	5.0089	5.5534
4.6229	4.7884	5.3107	4.6060	6.1544	5.6917	4.3209
4.7717	4.7373	4.8572	4.5580	5.3899	3.9027	4.2474
4.9816	4.7132	5.5777	5.2895	5.3506	3.5935	4.5390
5.8747	5.5149	5.2173	5.0405	4.4965	5.0615	4.9544
6.1415	5.6667	4.6282	4.9098	5.8044	6.1138	6.7215
<b>a</b>						
6.3531	6.5710	6.1352	6.2593	6.4436	6.3679	6.8031
6.3144	6.1222	6.8572	6.3285	6.2891	6.3459	6.9631
6.3738	6.8469	7.0577	6.3903	6.8603	6.9833	5.7541
6.6325	6.5823	7.7029	13.7060	7.0121	5.2678	6.0607
6.8448	6.9082	7.6694	8.7884	6.7205	5.7790	6.4054
6.6133	6.8105	6.3557	6.3543	6.2898	6.4478	6.8377
7.2528	6.4599	5.2150	6.4466	7.1746	7.0196	8.4101
<b>b</b>						
6.6627	6.1991	6.8938	7.1902	6.5414	7.2277	6.7772
5.8135	6.2246	6.9916	6.3754	7.1993	6.5661	6.4918
6.3745	7.6501	6.9468	7.5111	8.0919	7.0605	7.0526
5.8467	5.7724	6.1066	6.6417	5.6320	6.2556	5.7983
6.0745	5.5533	6.7050	6.7560	6.2486	7.0366	6.2248
5.6919	6.7364	7.2359	6.8283	7.6157	6.8558	6.8366
6.5099	7.0992	6.0692	5.8366	7.7806	7.1201	6.9752
<b>c</b>						

Fig. 10:  $\Delta T$  values around the first fire pixel detected by the proposed method indicated by a red rectangular on (a) July 24, (b) July 26 and (c) July 27 2006

323.1485	317.0161	318.9262	321.7707	322.7169	326.6881	325.1389
323.2734	318.6521	316.7132	317.8925	319.3035	320.7713	324.4988
317.0460	316.8950	318.6602	318.5176	319.2382	322.7471	323.5054
318.8077	318.8387	320.0159	323.5749	322.1294	322.5852	321.4995
318.3976	317.1227	320.2536	320.3518	319.2329	320.4678	320.8910
323.9287	319.2449	321.7359	318.7509	317.7090	318.5162	320.2782
325.8219	324.4598	325.2221	323.6349	321.3104	320.8312	323.0029
<b>a</b>						
319.9415	323.1211	317.8300	319.3726	321.0988	319.4906	322.8025
318.6127	321.8548	315.8495	315.8613	319.2636	319.8028	322.2335
319.3646	316.4899	318.6697	320.8147	317.9839	321.6975	323.0758
320.1577	318.4385	319.9924	333.7288	323.3102	323.0543	322.2017
321.4857	316.5260	318.9222	320.9760	319.9128	321.9708	320.6576
325.8418	321.9215	318.1108	320.9024	319.1595	319.2302	320.9215
328.4710	324.9977	322.7012	323.6772	320.4716	318.6344	320.2393
<b>b</b>						
322.0029	322.3032	318.6317	315.7330	315.5670	322.4116	324.7742
322.0914	320.1512	319.2476	315.1380	316.6140	323.8190	324.2721
322.9118	319.7161	317.4655	315.6516	317.8217	324.1657	323.6713
320.0354	316.4914	316.1982	318.5121	318.9975	321.4907	321.7595
316.4914	318.2579	318.3292	316.7591	317.3502	321.5544	321.5456
321.4757	320.5564	317.9617	316.0668	317.3784	323.0961	324.6739
322.0459	319.2982	316.2608	316.7203	317.3981	322.1564	322.3581
<b>c</b>						

Fig. 11:  $T_d$  values around the second fire pixel detected by the proposed method indicated by a red rectangular on (a) July 24, (b) July 26 and (c) July 27 2006

doesn't have major difference with respect to the surrounding. The  $\Delta T$  value of the given pixel in Fig. 10b can also be distinguished from the surrounding pixels, but not evidently in Fig. 10 a and c. For the second case, as can be shown in Fig. 11b, the contrast between  $T_d$  value

of the considered pixel and the neighbors is about 13 K on July 26 2006 but it is not noticeable in Fig. 11a and c. For  $\Delta T$ , it is about 10 K on July 26 2006 (Fig. 12b) but in Fig. 12a and c  $\Delta T$  values are comparable. Figure 6g and h show the results of the image taken on July 27, 2006 when

5.4348	4.2583	4.7532	5.7051	7.1326	9.8748	5.2606
5.1949	4.9778	3.8796	4.4387	4.6229	4.3788	4.5691
4.2287	3.8670	4.3320	3.9810	3.5216	4.4397	5.2968
4.0951	4.6336	4.1987	5.3248	4.7187	5.2215	4.5811
4.4013	3.7981	4.7594	5.0592	4.3019	4.7670	4.5195
4.6323	3.5918	4.6707	4.1610	3.9864	4.0224	4.3129
5.0930	4.4428	4.6313	4.5193	4.0147	4.1177	4.4567
<b>a</b>						
5.6668	6.4339	5.6142	6.9072	7.5051	5.2159	6.1100
5.1697	6.9291	4.8887	4.5336	5.9713	5.3838	5.6883
6.7584	5.7540	5.9551	6.9578	5.1017	5.5263	6.2677
5.5517	5.3835	6.9914	15.5826	6.5809	5.6906	5.8882
5.7161	4.9635	5.4038	6.3755	5.7451	6.6199	5.4129
5.3072	5.5764	4.7324	5.8118	5.2812	5.2983	5.6661
5.8741	6.1303	4.8832	5.3543	4.9669	4.6596	5.1434
<b>b</b>						
6.9335	8.0820	6.6387	6.2052	5.4697	7.0288	7.1126
7.4588	7.7400	6.7767	5.6823	5.4285	7.4001	7.1230
7.1898	7.0557	6.3349	6.0075	5.8342	7.4942	7.1629
6.9427	5.6402	5.6327	6.4213	6.1207	6.8368	6.4457
5.3224	5.2839	6.2492	5.8640	6.0609	6.7352	5.8978
6.6405	7.2642	6.1702	6.2069	5.9906	6.9407	7.3311
6.7905	6.9195	5.7173	5.9570	5.6066	6.9435	6.5091
<b>c</b>						

Fig. 12:  $\Delta T$  values around the second fire pixel detected by the proposed method indicated by a red rectangular on (a) July 24, (b) July 26 and (c) July 27 2006

three fire events were recorded by ground reconnaissance (Table 3, Fig. 6i). The reported fires happened in the evening. Notwithstanding the image was observed in the morning, both algorithms have detected one of the reported fires which based on field data, took place from 2:00 to 8:00 pm with 10 ha extent.

### DISCUSSION

In this study, we have tested an agent-based approach for regional forest fire detection with a series of MODIS images. As mentioned in lots of literatures (Ichoku *et al.*, 2003) by adapting fire detection algorithms to specific regional contexts, much accuracy improvement could be achieved regionally. Herein, agents encapsulate local and intelligent processing based upon tests used in the MODIS version 4 contextual algorithm (Giglio *et al.*, 2003). They sense and react to a small neighboring region of a number of pre-selected pixels. These pixels are identified based on brightness temperature and NDVI values of a given pixel with respect to those of its surrounding pixels rather than fixed threshold values as opposed to contextual fire detection algorithms (Giglio *et al.*, 2003). During the course of processing, if fire size exceeds a pixel, the considered agent will self-reproduce a number of off-springs to detect remaining fire-contaminated pixels. Indeed, the proposed algorithm was designed to be self-adaptive enough to be applied to any given image at regional scale. For the evaluation

purpose the proposed algorithm was compared with the MODIS version 4 contextual algorithm (Giglio *et al.*, 2003). Overall, the visual analysis of the results shows the potential of the proposed approach for fire detection using MODIS data. However, a pixel was detected as a fire event only by the proposed algorithm; it was excluded from computation using specified fixed threshold values for selection of potential fire pixels in the algorithm of Giglio *et al.* (2003). On the other hand, specification of optimum fixed threshold values is difficult especially in regional scale applications (Csiszar *et al.*, 2003; Giglio *et al.*, 2003; Li *et al.*, 2001, 2003; Wang *et al.*, 2007) and it is necessary to incorporate additional information to achieve more reliable results.

### CONCLUSION

This study proposed an agent-based approach for forest fire detection with MODIS imagery at regional scale. The algorithm is based on MODIS contextual fire detection algorithm (version 4). However, it uses spatial information surrounding image pixels for selection of potential fire pixels as well as detection of fire pixels. The results were compared with ground-based measurements and MODIS fire product (version 4). It shows high potential of the proposed algorithm for automatic forest fire detection at regional scale. In fact, it implies that without need to set any fixed threshold value for selection of potential fire pixels, it is possible to achieve good

results. Additional algorithm enhancements may be made in future. As an improvement based on our present study, we would investigate an agent-based approach to monitor forest fire events using multi-temporal images, in which one idea is introducing supplementary spatial and temporal tests to obtain more reliable results.

#### ACKNOWLEDGMENTS

We thank Forest, Range and Watershed Management Organization for providing ground-based measurements and Iranian Space Agency for providing MODIS data.

#### REFERENCES

- Byun, Y.G., Y. Huh, K. Yu and Y. Kim, 2005. Evaluation of graph-based analysis for forest fire detections. *World Acad. Sci. Eng. Technol.*, 10: 24-29.
- Csiszar, I., A. Abuelgasim, Z. Li, J.Z. Jin, R. Fraser and W.M. Hao, 2003. Interannual changes of active fire detectability in North America from long term records of the advanced very high resolution radiometer. *J. Geophys. Res.*, 108: ACL19.1-ACL19.10.
- Cuomo, V., R. Lasaponara and V. Tramutoli, 2001. Evaluation of a new satellite-based method for forest fire detection. *Int. J. Remote Sens.*, 22: 1799-1826.
- Giglio, L., J.D. Kendall and C.O. Justice, 1999. Evaluation of global fire detection algorithms using simulated AVHRR infrared data. *Int. J. Remote Sens.*, 20: 1947-1985.
- Giglio, L., J. Descloitres, C.O. Justice and Y. Kaufman, 2003. An enhanced contextual fire detection algorithm for MODIS. *Remote Sens. Environ.*, 87: 273-282.
- Ichoku, C., Y.J. Kaufman, L. Giglio, Z. Li, R.H. Fraser, J.Z. Jin and W.M. Park, 2003. Comparative analysis of daytime fire detection algorithms using AVHRR data for the 1995 fire season in Canada: perspective for MODIS. *Int. J. Remote Sens.*, 24: 1669-1690.
- Justice, C.O., L. Giglio, S. Korontzi, J. Owens, J.T. Morisette, D. Roy, J. Descloitres *et al.*, 2002. The MODIS fire product. *Remote Sens. Environ.*, 83: 244-262.
- Kaufman, Y.J., C.O. Justice, L.P. Flynn, J.D. Kendall, E.M. Prins, L. Giglio and D.E. Ward *et al.*, 1998. Potential global fire monitoring from EOS-MODIS. *J. Geophys. Res.*, 103: 32215-32238.
- Keshkar, F. and W. Gueaieb, 2006. Conventional and agent-based image segmentation algorithms: A comparative study. *Proceedings of the 11th International CSI Computer Conference, IPM, Tehran, Iran, January 2006.*
- Lentile, L.B., Z.A. Holden, A.M.S. Smith, M.J. Falkowski and A.T. Hudak *et al.*, 2006. Remote sensing techniques to assess active fire characteristics and post-fire effects. *Int. J. Wildland Fire*, 15: 319-345.
- Li, Z., Y. Kaufman, C. Ichoku, R. Fraser, A. Trishchenko, L. Giglio, J.Z. Jin and X. Yu, 2001. A Review of Avhrr-Based Active Fire Detection Algorithms: Principles, Limitations and Recommendations. In: *Regional Vegetation Fire Monitoring from Space: Planning a Coordinated International Effort*, Ahern, F., Goldammer, J.G. and Justice, C. Global (Eds.), SPB Academic Publishing, Hague/Netherlands, pp: 199-225.
- Li, Z., R. Fraser, J. Jin, A.A. Abuelgasim, I. Csiszar, P. Geng, R. Pu and W. Hao, 2003. Evaluation of algorithms for fire detection and mapping across North America from satellite. *J. Geophys. Res.*, 108: ACL20.1-ACL20.14.
- Li, Y., A. Vodacek, R.L. Kremens, A. Ononye and C. Tang, 2005. A hybrid contextual approach to wildland fire detection using multispectral imagery. *IEEE Trans. Geosci. Remote Sens.*, 43: 2115-2126.
- Liu, J. and Y.Y. Tang, 1998. Distributed autonomous agents for Chinese document image segmentation. *Int. J. Pattern Recognit. Artifi. Intell.*, 12: 97-118.
- Liu, J. and Y.Y. Tang, 1999. Adaptive image segmentation with distributed behavior-based agents. *IEEE Trans. Pattern Anal. Mach. Intell.*, 21: 544-551.
- Maes, P., 1994. Modeling adaptive autonomous agents. *Artificial Life J.*, 1: 135-162.
- Robinson, J.M., 1991. Fire from space: Global fire evaluation using infrared remote sensing. *Int. J. Remote Sens.*, 12: 3-24.
- Wang, W., J.J. Qu, Y. Liu, X. Hao and W. Sommers, 2007. An improved algorithm for small and cool fire detection using MODIS data: A preliminary study in the Southern United States. *Remote Sens. Environ.*, 108: 163-170.